ЖУРНАЛ СТРУКТУРНОЙ ХИМИИ

2015. Том 56, № 8 *Декабрь* *С. 1545 – 1556*

UDC 541.49:546.93:541.67

SUBSTITUENT AND SOLVENT EFFECTS ON GEOMETRIC AND ELECTRONIC STRUCTURE OF $C_5H_5Ir(PH_3)_3$ IRIDABENZENE: A THEORETICAL INSIGHT

R. Ghiasi, E. Amini

Department of Chemistry, Faculty of Basic Science, East Tehran Branch, Islamic Azad University, Qiam Dasht, Tehran, Iran
E-mail: rezaghiasi1353@yahoo.com; rghiasi@iauet.ac.ir

Received October, 22, 2014

Using MPW1PW91 quantum chemical calculations, we report structures, frontier orbital analysis, natural bond analysis, and aromaticity of the $C_5H_5Ir(PH_3)_3$ iridabenzene and $XC_5H_4Ir(PH_3)_3$ *para*-substituted iridabenzenes. The substituent effects were estimated from the donor—acceptor interaction energies of the natural bond orbitals of substituent and iridabenzene frame. Nucleus-independent chemical shift (NICS) has been evaluated to understand the aromaticity. Time dependent density functional theory (TD-DFT) is used to calculate the energy, oscillatory strength and wavelength absorption maxima (λ_{max}) of electronic transitions and their nature. Changes in hyperpolarizability of molecules are studied. Influence of solvent on the structure, frontier orbital energies, λ_{max}, and hyperpolarizability of $C_5H_5Ir(PH_3)_3$ iridabenzene has been studied.

DOI: 10.15372/JSC20150805

K e y w o r d s: iridabenzene, substituent effect, solvent effect, natural bond orbital (NBO) analysis, nucleus independent chemical shift (NICS), hyperpolarizability.

INTRODUCTION

Metallacyclic aromatic compounds including transition metals are subject of great attention, because they exhibit a behavior that includes properties resulting from both aromatic organic and organometallic compounds. For example, metallabenzenes are six-membered metallacycles analogous to benzene in which one CH unit has been replaced by an isolobal transition-metal fragment [ML_n]. A significant number of papers have appeared that address the synthesis and properties of metallabenzenes [1—6]. For example, a transition metal incorporated into stable metallabenzene complexes is iridium. Synthesis of a series of iridabenzenes has been reported [7—10]. In contrast to the situation with simple metallabenzenes, where there is now an extensive amount of related synthetic, structural, spectral, computational, and reactivity data available [1—3, 11—16], examples of heterocyclic ring metallabenzenes are scarce [17]. For example, synthesis and properties of with metallabenzofuran [18, 19], metallabenzothiophene [19], metallabenzothiazolium [20] metallabenzothiazole [21] and metallabenzoxazole [21] have been reported.

In the present study, the geometries, aromaticity, solvent effect and substitution effect of iridabenzene $C_5H_5Ir(PH_3)_3$ are investigated. Natural bond orbital analysis (NBO) provides detailed insight into the electronic structure of molecules.

COMPUTATIONAL METHODS

All calculations were carried out with the Gaussian 03 suite of program [22]. The calculations of systems contain C, N, H, O, F, Cl, Br, and P described by the standard 6-311G(*d*,*p*) basis set [23—26]. For Ir element standard LANL2DZ basis set [27—29] are used and Ir described by effective core potential (ECP) of Wadt and Hay pseudopotential [27] with a doublet-ξ valence using the LANL2DZ. Geometry optimization was performed utilizing with Modified Perdew-Wang Exchange and Correlation (MPW1PW91) [30]. Vibrational analysis was performed at each stationary point found, to confirm its identity as an energy minimum.

The population analysis has also been performed by the natural bond orbital method [31] using NBO program [32] with Gaussian 2003 program package.

The nucleus-independent chemical shift (NICS) index, based on the magnetic criterion of aromaticity, is probably the most widely used probe for examination of chemical compounds aromatic properties [33]. It is defined as the negative value of the absolute magnetic shielding. It can be calculated in the centre of the aromatic ring (NICS(0) [34]), or at 1 Å above it (NICS(1) [35]). Negative NICS values denote efficient electron delocalization. Nucleus-independent chemical shifts were calculated in the point located by 1 Å above the center of the ring (NICS(1)*zz*) as it was recommended for obtaining more accurate data [36, 37]. NICS values are calculated using the Gauge independent atomic orbital (GIAO) [38] method at the same method and basis sets for optimization.

The information of the MOs was evaluated by total, partial and overlap population density of states (DOS) using the GaussSum 2.2 software package [39]; the full width at half maximum (FWHM) of 0.3 eV was used to convolute the spectrum.

Geometries were optimized at this level of theory without any symmetry constraints followed by the calculations of the first order hyperpolarizabilities. The total static first hyperpolarizability β was obtained from the relation:

$$\beta_{\text{tot}} = \sqrt{\beta_x^2 + \beta_y^2 + \beta_z^2}$$

upon calculating the individual static components

$$\beta_i = \beta_{iii} + \frac{1}{3}\sum_{i \neq j}(\beta_{ijj} + \beta_{jij} + \beta_{jji}).$$

Due to the Kleinman symmetry [40]:

$$\beta_{xyy} = \beta_{yxy} = \beta_{yyx}; \quad \beta_{yyz} = \beta_{yzy} = \beta_{zyy}, \ldots$$

one finally obtains the equation that has been employed:

$$\beta_{\text{tot}} = \sqrt{(\beta_{xxx} + \beta_{xyy} + \beta_{xzz})^2 + (\beta_{yyy} + \beta_{yzz} + \beta_{yxx})^2 + (\beta_{zzz} + \beta_{zxx} + \beta_{zyy})^2}.$$

The electronic spectra for the studied compounds were calculated by TD-DFT [41] using the same hybrid functionals and basis sets as used for the calculation of the hyperpolarizabilities. The 10 lowest excitation energies were computed.

For the solvation effects study we have used a self-consistent reaction field (SCRF) approach, in particular using the polarizable continuum model (PCM) [42]. With this method, the geometry of the studied complex was re-optimized and the UV/Vis spectrum was calculated by DFT/TD-DFT with the same functionals and basis sets.

RESULTS AND DISCUSSION

Energy. Fig. 1 presents the molecular structure and atomic numbering of $C_5H_5Ir(PH_3)_3$ iridabenzene. The energies of $C_5H_5Ir(PH_3)_3$ in gas phase and in different media calculated by using the PCM model are listed in Table 1. E_T is the total energy and ΔE_{solv} is the stabilization energy by solvents, the energy of the title compound in a solvent relative to that in the gas phase.

From Table 1, we can see that the calculated energy is dependent on the dielectric constant of solvents. In the PCM model, the energies E_T decrease with the increasing dielectric constants. On the other hand, ΔE_{solv} values indicate to increase in the stability in more polar solvents. This is because a dipole in the molecule will induce a dipole in the medium, and the electric field applied to the solute

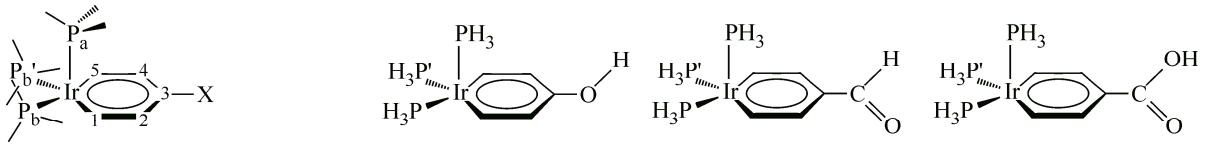

Fig. 1. Structures of studied *para*-substituted iridabenzenes

T a b l e 1

Dielectric constants of solvents (ε), *Absolute energy* (*E*, Hartree), *dipole moment* (μ, Debye) *values, and solvent stabilization energies* (ΔE_{solv}, kcal/mol) *values for* $C_5H_5Ir(PH_3)_3$ *iridabenzene in various solvent*, *and Absolute energy* (Hartree), *Hammet constants and dipole moment* (Debye) *values for iridabenzene and para-substituted iridabenzenes in vacuum*

	ε	*E*	μ	ΔE_{solv}	X	σ_p	*E*	μ
Gas	—	–1327.8050	4.37	—	H	0.00	–1327.8050	4.37
$CHCl_3$	4.71	–1327.8142	6.83	–5.73	F	0.06	–1427.0532	5.72
Chlorobenzene	5.70	–1327.8150	7.06	–6.27	Cl	0.23	–1787.4407	6.68
Aniline	6.89	–1327.8158	7.27	–6.76	Br	0.23	–3901.5163	6.74
THF	7.43	–1327.8161	7.35	–6.93	OH	–0.37	–1403.0374	3.68
CH_2Cl_2	8.93	–1327.8167	7.52	–7.34	NH_2	–0.66	–1383.1736	1.01
Quinoline	9.16	–1327.8168	7.55	–7.39	Me	–0.17	–1367.1242	3.85
Isoquinoline	11.00	–1327.8174	7.70	–7.74	CN	0.66	–1420.0485	10.38
					NO_2	0.78	–1532.3171	10.79
					CHO	0.42	–1441.1332	8.73
					COOH	0.45	–1516.3908	7.06

by the solvent (reaction) dipole will in turn interact with the molecular dipole to lead to net stabilization. This suggests that the $C_5H_5Ir(PH_3)_3$ iridabenzene has more stability in a polar solvent rather than in the gas phase.

Dipole moments. Dipole moment values of $C_5H_5Ir(PH_3)_3$ in gas phase and in different media by using the PCM model are listed in Table 1. These values show that the solvent effect on the stabilization energy parallels that on the dipole moment of the solute. There is a good linear relationship between the solvent stabilization energies and the dipole moments of $C_5H_5Ir(PH_3)_3$ in the set of solvents with the correlation coefficient of 1.00. The larger is the dipole moment of solute, and the higher is the stabilization energy in more polar solvent. There is a good correlation between dipole moment and dielectric constant with the correlation coefficient of 0.935.

The *para*-substituted iridabenzenes and their arbitrary numbering are presented in Fig. 1. Absolute energies, dipole moments of *para*-substituted iridabenzenes and Hammett constants values are gathered in Table 1. As seen from Table 1, dipole moment values increase with increasing Hammett constants. A good correlation is observed between dipole moments and Hammett constants (Fig. 2).

Structural parameters. The selected bond distances in $C_5H_5Ir(PH_3)_3$ are collected in Table 2. It is well-known that the solvent polarity influences both the structure and properties of conjugated organic molecules and metal complexes [43—45]. The structural data for the optimized

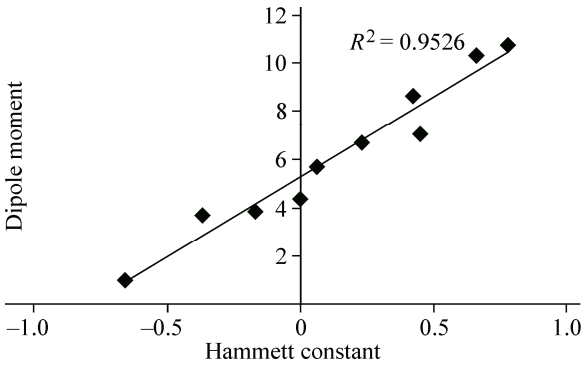

Fig. 2. A linear correlation between dipole moments and Hammett constants for substituted iridabenzenes

Table 2

Bond distances (Å) *in* $C_5H_5Ir(PH_3)_3$ *in various solvents for iridabenzene and para-substituted iridabenzenes in vacuum*

X	Ir—C1	C1—C2	C2—C3	C3—C4	C4—C5	C5—Ir	Ir—P_{ax}	Ir—P_{eq}	Ir—P'_{eq}
Gas	1.9881	1.3826	1.3917	1.3917	1.3826	1.9881	2.2593	2.3432	2.3432
$CHCl_3$	1.9874	1.3859	1.3930	1.3930	1.3859	1.9874	2.2637	2.3531	2.3531
Chlorobenzene	1.9873	1.3862	1.3931	1.3931	1.3862	1.9873	2.2642	2.3540	2.3540
Aniline	1.9873	1.3864	1.3932	1.3932	1.3864	1.9873	2.2647	2.3548	2.3548
THF	1.9873	1.3865	1.3933	1.3933	1.3865	1.9873	2.2649	2.3550	2.3550
CH_2Cl_2	1.9873	1.3867	1.3934	1.3934	1.3867	1.9873	2.2654	2.3557	2.3557
Quinoline	1.9872	1.3868	1.3934	1.3934	1.3868	1.9872	2.2654	2.3558	2.3558
Isoquinoline	1.9872	1.3869	1.3935	1.3935	1.3869	1.9872	2.2658	2.3563	2.3563
H	1.9881	1.3826	1.3917	1.3917	1.3826	1.9881	2.2593	2.3432	2.3432
F	1.9887	1.3807	1.3858	1.3858	1.3807	1.9887	2.2685	2.3401	2.3401
Cl	1.9855	1.3816	1.3898	1.3898	1.3816	1.9855	2.2644	2.3435	2.3435
Br	1.9852	1.3823	1.3901	1.3901	1.3823	1.9852	2.3441	2.2635	2.2635
OH	1.9954	1.3744	1.3976	1.3959	1.3794	1.9866	2.2751	2.3353	2.3348
NH_2	1.9938	1.3734	1.4060	1.4060	1.3734	1.9938	2.2795	2.3309	2.3309
Me	1.9873	1.3805	1.3976	1.3976	1.3805	1.9873	2.263	2.3408	2.3408
CN	1.9862	1.3790	1.4007	1.4007	1.3790	1.9862	2.2542	2.3501	2.3501
NO_2	1.9867	1.3797	1.3901	1.3901	1.3797	1.9867	2.2497	2.3523	2.3523
CHO	1.9957	1.3744	1.4004	1.3948	1.3823	1.9837	2.2498	2.3502	2.3501
COOH	1.9886	1.3778	1.3980	1.3973	1.3810	1.9859	2.2503	2.3494	2.3494

structures of $C_5H_5Ir(PH_3)_3$ in the seven studied solvents are compiled in Table 2. The results show that the structural parameters are changed with the polarity of the surrounding media. These values indicate shortening of the Ir—C, Cr—C_{cis}, and lengthening of the Ir—P, C—C bonds in solvents rather than in gas phase.

Introduction of electron withdrawing substituents results in a decrease of the Ir—P_{ax} bond length and a lengthening of the Ir—P_{eq} bond, with respect to the corresponding parameters of the unsubstituted iridabenzene molecule. On the other hand, Ir—C bonds are longer in the presence of the electron withdrawing rather than electron-donating substituents. The C1—C2 bond lengths decrease the substituted rather than unsubstituted molecules. The C2—C3 bonds distances decrease in the presence of halogens, but increase with other substituents.

Although theoretical results are not exactly close to the experimental values [46] for the title molecule, this may be due to the fact that the theoretical calculations were aimed at the isolated molecule in gaseous phase and the experimental results refer to the solid state. The calculated geometric parameters represent good approximation and they can be used as foundation to calculate the other parameters for the compound.

Bond order. Wiberg bond orders of iridabenzene and *para*-substituted iridabenzenes have been computed (Table 3). For the electron donor substitutions (X = F, Cl, Br, Me, NH_2, OH), we note that bonding is more covalent. On the other hand, bond covalency in iridabenzene ($\sum$BOR = 7.89) is higher than in *para*-substituted iridabenzenes.

Frontier orbitals energy. The influence of substituent nature is reflected not only in the geometric parameters of the molecules, but also in the energies of frontier orbitals. It is well-known that the frontier orbitals energy and HOMO-LUMO gap values are closely related to the optical and electronic properties.

Inclusion of solvation effects also leads to changes in the molecular orbital energies (Table 4). In solution frontier orbitals are stabilized with respect to the corresponding values in vacuum. On the other hand, the HOMO-LUMO gaps in solvating media are higher than in vacuum.

Table 3

Wiberg indexes for iridabenzene and para-substituted iridabenzenes

X	Ir—C1	C1—C2	C2—C3	C3—C4	C4—C5	C5—Ir	∑B.O
H	1.055	1.505	1.388	1.388	1.505	1.055	7.897
F	1.050	1.508	1.350	1.350	1.509	1.050	7.817
Cl	1.054	1.497	1.356	1.356	1.497	1.054	7.814
Br	1.055	1.493	1.365	1.365	1.493	1.055	7.827
OH	1.017	1.555	1.296	1.322	1.515	1.048	7.753
NH_2	1.015	1.560	1.276	1.276	1.561	1.014	7.702
Me	1.048	1.514	1.349	1.348	1.515	1.047	7.820
CN	1.051	1.519	1.312	1.312	1.519	1.051	7.764
NO_2	1.050	1.511	1.335	1.335	1.511	1.050	7.794
CHO	1.022	1.554	1.297	1.340	1.498	1.068	7.779
COOH	1.043	1.526	1.323	1.334	1.512	1.055	7.792

Table 4

Frontier orbital energies (a.u.), *frontier orbitals gap* (eV), *hardness*, *softness* (1/eV), *chemical potential* (eV) *and electrophilicity* (eV) *values for studied iridobenzene in various solvents and para-substituted iridabenzenes in vacuum*

X	HOMO	LUMO	ΔE	η	S	μ	ω
Gas	–0.1838	–0.0481	3.694	1.85	0.54	–3.16	2.69
$CHCl_3$	–0.1884	–0.0510	3.741	1.87	0.54	–3.26	2.83
Chlorobenzene	–0.1890	–0.0513	3.746	1.87	0.53	–3.27	3.85
Aniline	–0.1896	–0.0517	3.752	1.88	0.53	–3.28	3.87
THF	–0.1898	–0.0519	3.754	1.88	0.53	–2.29	2.89
CH_2Cl_2	–0.1903	–0.0522	3.759	1.88	0.53	–2.30	2.90
Quinoline	–0.1904	–0.0522	3.760	1.88	0.53	–3.30	2.90
Isoquinoline	–0.1909	–0.0525	3.764	1.88	0.53	–3.31	2.91
H	–0.1838	–0.0481	3.69	1.85	0.54	–3.15	2.69
F	–0.1862	–0.0489	3.74	1.89	0.54	–3.20	2.74
Cl	–0.1901	–0.0566	3.63	1.82	0.55	–3.36	3.10
Br	–0.1902	–0.0575	3.61	1.81	0.55	–3.37	3.14
OH	–0.1754	–0.0392	3.71	1.85	0.54	–2.92	2.30
NH_2	–0.1641	–0.0309	3.63	1.81	0.55	–2.65	1.94
Me	–0.1802	–0.0452	3.67	1.84	0.54	–3.06	2.56
CN	–0.2015	–0.0763	3.40	1.70	0.59	–3.78	4.19
NO_2	–0.2055	–0.0865	3.24	1.62	0.62	–3.97	4.87
CHO	–0.1968	–0.0762	3.28	1.64	0.61	–3.71	4.20
COOH	–0.1942	–0.0700	3.38	1.69	0.59	–3.59	3.82

To get insight into the influence on the optical and electronic properties, the distributions of the frontier orbitals were investigated, and their sketches are plotted in Fig. 3. Molecular orbital analysis shows that HOMO and LUMO are of the π character, as visualized in Fig. 3. Frontier orbital analysis presents the HOMO as distributed over all atoms of the molecule. On the other hand, LUMO is distributed over Ir, C and the axial phosphine ligand.

Total density of states (DOS), and overlap population density of state (OPDOS) of iridabenzene are presented in Fig. 3. These spectra provide graphical representation of MO compositions and their contributions to chemical bonding, and the OPDOS spectra can help us to analyze the bonding (posi-

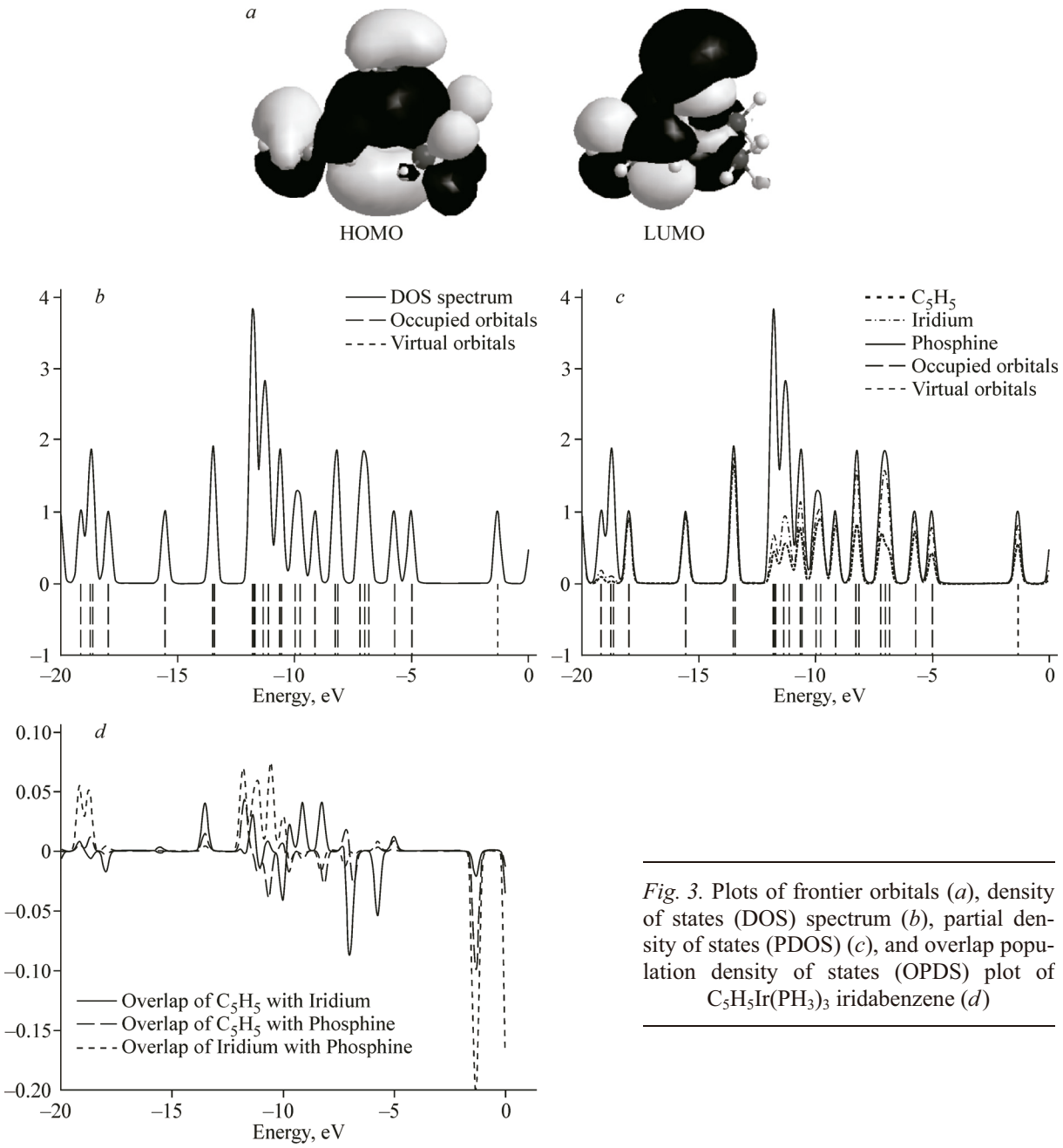

Fig. 3. Plots of frontier orbitals (*a*), density of states (DOS) spectrum (*b*), partial density of states (PDOS) (*c*), and overlap population density of states (OPDS) plot of $C_5H_5Ir(PH_3)_3$ iridabenzene (*d*)

tive value), antibonding (negative value), and nonbonding (near zero value) characters with respect to the particular fragments.

Plotting the energies of the frontier orbitals of the molecules is shown in Fig. 4. The linear interpolation of the data points corresponding yields correlation coefficients of 0.935 (Fig. 4). Therefore, the HOMO or the LUMO are similar in topology for different substituents.

Another way to recognize the influence on the optical and electronic properties is to analyze the *E*(HOMO), *E*(LUMO), and HOMO-LUMO gap values (Table 3). We calculated the frontier orbitals energies of all the molecules. These values indicate that *E*(HOMO) values increase when X = Me, NH, OH. *E*(HOMO) values for electron donor groups are higher than for withdrawing electron groups. On the other hand, *E*(LUMO) values increase in X = Me, NH, OH substituted molecules. There is larger *E*(LUMO) values for electron donating groups than for withdrawing groups. A good linear relation is seen between frontier orbitals energy and Hammett constants (Fig. 5).

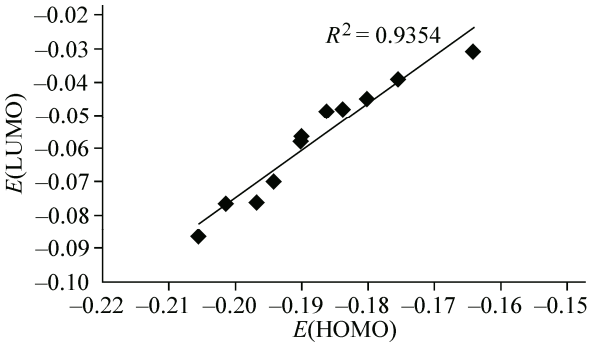

Fig. 4. A linear correlation between HOMO and LUMO energies for substituted iridabenzenes

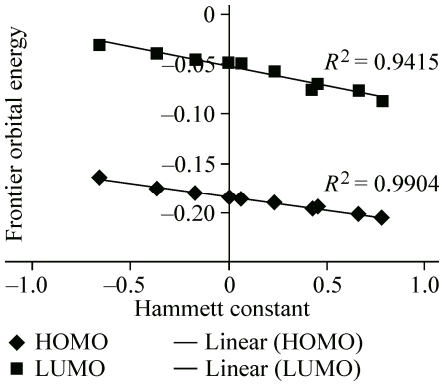

Fig. 5. A linear correlation between frontier energies and Hammett constants for substituted iridabenzenes

The effect of the substitution on the hardness values shows decrease of these values in substituted molecules (except X = F). The highest hardness values are found for electron donor groups.

The study of the effect of the substitution on the chemical potential values shows increasing these values with increasing Hammett constants. On the other hand, electrophilicity values decrease with increasing Hammett constants. As seen in Fig. 6, there is a good correlation between chemical potential, electrophilicity values, and Hammett constants.

Nucleus Independent Chemical Shift analyses (NICS). NICS is an easy and efficient criterion to identify aromatic nature. A large negative NICS at the ring center (or inside and above the molecular plane) implies the presence of diamagnetic ring currents. As shown in Fig. 7, all the computed NICS(0.0) values at the geometrical center of cycles are in the range of –4.5 ppm to –7.8 ppm, suggesting that these molecules are clearly aromatic. In order to further identify the aromaticity of the molecules, we calculated the NICS values (including NICS(0.5), NICS(1.0), NICS(1.5), and NICS(2.0)) by placing a series of ghost atoms above (by 0.5 Å, 1.0 Å, 1.5 Å, 2.0 Å) the geometrical centers. All these NICS values are mainly attributed to the delocalized π electrons current. The most negative of these values are 1.0 Å above of the ring center. In addition, we focused on the $NICS(1)_{zz}$ index to explain the variation of the degree of aromaticity in all ring. Fig. 7 presents a good correlation between NICS(1.0) and $NICS(1.0)_{zz}$ values and Hammett constants for withdrawing electron groups (X = Cl, Br, CN, NO_2, CHO, COOH) (Table 5).

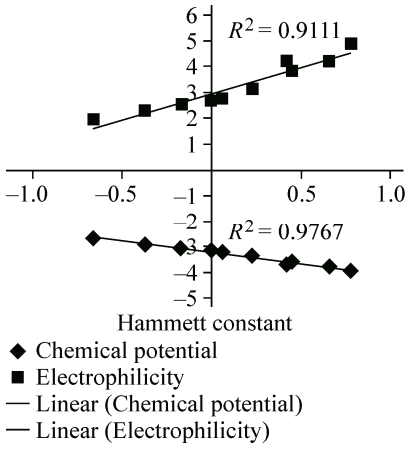

Fig. 6. A linear correlation between chemical potential and electrophilicity with Hammett constants for substituted iridabenzenes

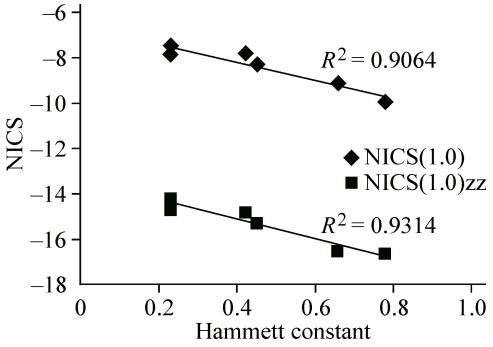

Fig. 7. A linear relationship between NICS(1.0) and NICS(1.0)zz values and Hammett constants for X = Cl, Br, CN, NO_2, CHO, COOH

Table 5

The NICS(0.0), NICS(0.5), NICS(1.0), NICS(1.5), NICS(2.0) *and* $NICS(1.0)_{zz}$ (ppm) *values for para-substituted iridabenzenes*

X	NICS(0.0)	NICS(0.5)	NICS(1.0)	NICS(1.5)	NICS(2.0)	$NICS(1.0)_{zz}$
H	–4.36	–4.74	–6.72	–6.48	–4.97	–13.28
F	–7.83	–8.84	–9.12	–7.17	–4.96	–15.82
Cl	–5.96	–6.89	–7.86	–6.61	–4.75	–14.72
Br	–5.59	–6.40	–7.50	–6.42	–4.65	–14.25
OH	–7.05	–7.96	–8.28	–6.55	–4.59	–13.91
NH_2	–4.70	–5.55	–6.35	–5.37	–3.97	–10.80
Me	–6.46	–7.85	–8.71	–7.07	–4.98	–15.71
CN	–6.96	–8.23	–9.14	–7.45	–5.21	–16.51
NO_2	–8.14	–9.29	–9.93	–7.93	–5.50	–16.65
CHO	–4.97	–6.25	–7.80	–6.77	–4.94	–14.86
COOH	–5.80	–6.95	–8.34	–7.13	–5.14	–15.35

Table 6

Atomic charge, *Natural Electron Configuration*, *number of electrons*, *and* $\sum E$ *values* (kcal/mol) *characterizing the nature of the substituents for para-substituted iridabenzene complexes*

X	*q*(Ir)	Natural electron configuration	# electrons	$\sum E$
H	–1.30029	[core]6*s*(0.47)5*d*(8.47)6*p*(1.37)6*d*(0.02)	78.33	—
F	–1.31999	[core]6*s*(0.47)5*d*(8.48)6*p*(1.38)6*d*(0.02)	78.35	38.55
Cl	–1.29725	[core]6*s*(0.47)5*d*(8.47)6*p*(1.36)6*d*(0.01)	78.31	26.9
Br	–1.29366	[core]6*s*(0.47)5*d*(8.47)6*p*(1.36)6*d*(0.01)	78.31	21.72
OH	–1.34302	[core]6*s*(0.46)5*d*(8.50)6*p*(1.38)6*d*(0.02)	78.36	44.42
NH_2	–1.36063	[core]6*s*(0.46)5*d*(8.51)6*p*(1.39)6*d*(0.02)	78.38	77.72
Me	–1.31183	[core]6*s*(0.47)5*d*(8.48)6*p*(1.37)6*d*(0.02)	78.51	14.65
CN	–1.24905	[core]6*s*(0.47)5*d*(8.44)6*p*(1.34)6*d*(0.01)	78.26	–30.02
NO_2	–1.23157	[core]6*s*(0.47)5*d*(8.44)6*p*(1.33)6*d*(0.01)	78.25	–32.4
CHO	–1.24102	[core]6*s*(0.47)5*d*(8.44)6*p*(1.33)6*d*(0.01)	78.25	–3.48
COOH	–1.25001	[core]6*s*(0.47)5*d*(8.44)6*p*(1.34)6*d*(0.01)	78.26	–2.77

Natural bond orbital analysis (NBO). According to the NBO results, the electron configuration of Ir is [core]6*s*(0.47)5*d*(8.47)6*p*(1.37)6*d*(0.02) for iridabenzene. Thus there are 10.33 valence electrons. This is consistent with the calculated natural charge on Ir atom (–1.300) which corresponds to the difference between 10.336 e and the total number of electrons in the isolated Ir atom (9). The electron configuration of Ir in *para*-substituted iridabenzenes is given in Table 6. Again, these values are consistent with the calculated natural charge on Ir atom (Table 6).

The stabilization energy *E*(2) is estimated by second order perturbation theory in terms of NBO analysis. The energy of electron-donating interactions was taken into account with the sign ″+″, and that of electron-accepting interactions with the sign ″–″. If $\sum E$ is negative, then the transfer of electron density from the benzene ring to the substituent dominates, i.e., the substituent is an acceptor, and vice versa. Table 6 lists the cooperative energetic characteristic of inductive and mesomeric effects of the iridabenzene and *para*-substituted iridabenzenes. Fig. 8 shows a clear correlation between the $\sum E$ and Hammett constants.

Electronic spectra. We found the most intense electronic transition wavelength (λ_{max}) of the molecules. The wavelength, oscillator strength and the composition of the transitions obtained by TD-DFT calculations are given in Table 7.

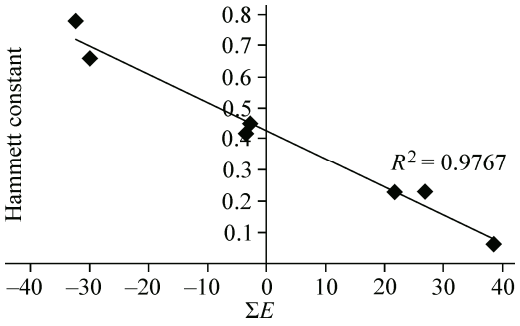

Fig. 8. A linear relationship between $\sum E$ and Hammett constant for X = F, Cl, Br, CN, NO_2, CHO, COOH

The calculations indicate that in $C_5H_5Ir(PH_3)_3$ HOMO → LUMO+4 transition makes the major contribution into this electronic transition.

Inclusion of solvation effects leads to changes of λ_{max} (Table 7). In solution, the λ_{max} is blue-shifted with respect to the corresponding values in vacuum. On the other hand, the λ_{max} value increases with increasing polarity of solvent. There is a good relationship between dielectric constant and λ_{max} as: $\lambda_{max} = -0.844\varepsilon + 257.3$; $R^2 = 0.936$.

The λ_{max} is a function of substituent. The more electron are pushed into the molecule the longer λ_{max} become.

Hyperpolarizability. The solvent polarity plays an important role in the first hyperpolarizabilities in dipolar molecules.

The β_{tot} values of $C_5H_5Ir(PH_3)_3$ in various solvents have been gathered in Table 8. These values indicate that β_{tot} values increase from vacuum to solution phase. The dependence of the first hyperpolarizability both on the dielectric constant of the media and the Onsager function can be seen [47]. Fig. 9 is typical for a dipolar reaction field interaction in the solvation process [47—50]. Therefore, the electronic reorganization in solution for $C_5H_5Ir(PH_3)_3$ exercises a significant effect on the first hyperpolarizabilities.

The β_{tot} values of iridabenzene and *para*-substituted iridabenzenes have been gathered in Table 7. These values indicate higher β_{tot} values for electron donor groups.

T a b l e 7

The wavelength, oscillator strengths, the composition of the maximum electronic transitions for $C_5H_5Ir(PH_3)_3$ *in various solvents; for iridabenzene and substituted iridabenzenes in vacuum*

Phase	Transition	λ_{max}	*f*	$\beta_{tot}\times10^{30}$
Gas	HOMO → LUMO+4	258.93	0.1049	11.83
$CHCl_3$	HOMO → LUMO+4	253.17	0.1478	20.35
Chlorobenzene	HOMO → LUMO+4	252.61	0.1524	21.01
Aniline	HOMO → LUMO+4	251.96	0.1517	21.52
thf	HOMO → LUMO+4	251.09	0.1370	21.69
CH_2Cl_2	HOMO → LUMO+4	250.42	0.1326	22.04
Quinoline	HOMO → LUMO+4	248.75	0.0969	22.08
Isoquinoline	HOMO → LUMO+4	248.18	0.0946	22.36
X				
F	HOMO → LUMO+4	258.79	0.1079	—
Cl	HOMO → LUMO+4	258.27	0.1093	—
Br	HOMO-2 → LUMO	295.53	0.1296	—
OH	HOMO → LUMO+4	266.43	0.1271	—
NH_2	HOMO → LUMO+4	275.41	0.1626	—
Me	HOMO → LUMO+4	261.72	0.1191	—
CN	HOMO-2 → LUMO	299.07	0.1802	—
NO_2	HOMO-2 → LUMO	307.92	0.2067	—
CHO	HOMO-3 → LUMO	304.07	0.1593	—
COOH	HOMO-2 → LUMO+1	299.35	0.1665	—

Table 8

β *Components and* β_{tot} *values* (10^{-30} esu) *for substituted iridabenzenes*

Parameter	H	F	Cl	Br	OH	NH_2
β_{xxx}	330.38	–658.36	–988.05	–1196.53	–772.57	–949.80
β_{xxy}	–0.65	–1.50	–0.82	–0.56	46.75	–0.97
β_{xyy}	516.28	–473.96	–528.43	–556.70	–478.61	–495.21
β_{yyy}	0.10	–0.54	–0.70	–0.30	48.23	0.73
β_{xxz}	–204.99	–168.60	–115.85	–90.17	–182.15	–252.47
β_{xyz}	–0.17	–0.66	0.34	0.31	–8.36	–0.80
β_{yyz}	–232.89	–260.29	–247.54	–247.84	–280.23	–310.10
β_{xzz}	409.55	–477.42	–580.97	–617.82	–549.82	–603.24
β_{yzz}	–0.06	–0.51	–0.16	–0.83	–88.17	–2.08
β_{zzz}	981.57	960.42	884.46	859.90	1084.24	1208.04
β_{tot}	1.18E—29	1.46E—29	1.87E—29	2.10E—29	1.65E—29	1.86E—29
$\beta_{tot}\times10^{30}$	11.83	14.65	18.67	20.98	16.46	18.55
Parameter	Me	CN	NO_2	CHO	COOH	
β_{xxx}	–455.49	–218.85	1574.54	–783.59	721.61	
β_{xxy}	2.30	0.11	–5.58	–194.81	26.08	
β_{xyy}	–509.47	–561.11	–622.06	543.22	–621.25	
β_{yyy}	0.96	–2.58	–12.69	13.31	27.44	
β_{xxz}	–195.14	–94.20	–132.28	–142.27	–136.72	
β_{xyz}	–0.20	0.43	0.07	1.06	–3.20	
β_{yyz}	–271.16	–211.43	–195.82	–213.17	–218.06	
β_{xzz}	–511.34	–583.75	–562.47	577.96	–581.88	
β_{yzz}	–4.58	–1.22	–5.09	85.15	–9.85	
β_{zzz}	985.31	766.33	704.10	766.42	774.31	
β_{tot}	1.35E—29	1.24E—29	4.68E—30	4.67E—30	5.53E—30	
$\beta_{tot}\times10^{30}$	13.52	12.44	4.68	4.67	5.53	

CONCLUSIONS

Gas and solvent phase theoretical calculations on $C_5H_5Ir(PH_3)_3$ iridabenzene indicate the increasing stability in polar solvents. In the basis of molecular orbital analysis, frontier orbitals are stabilized, with respect to the corresponding values in vacuum. Also, λ_{max} value and first hyperpolarizability increase with increasing dielectric constant of the media. On the other hand, the *para* substituent effect

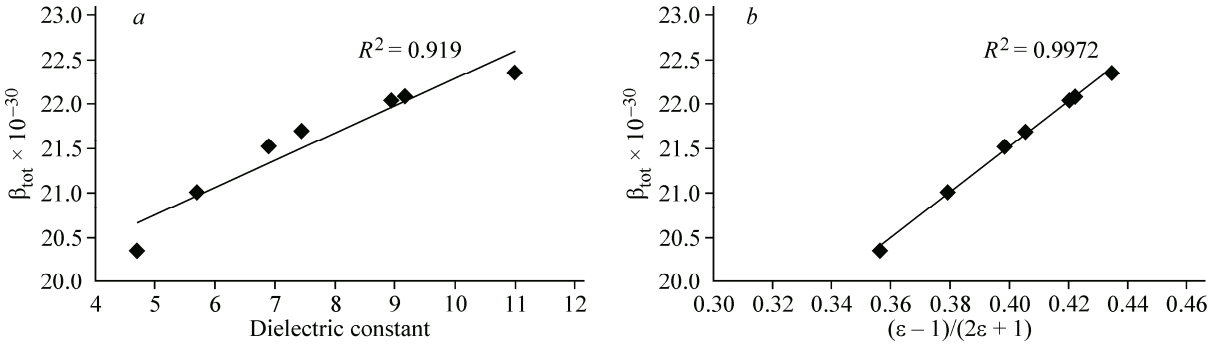

Fig. 9. Dependence of β for $C_5H_5Ir(PH_3)_3$ iridabenzene on the dielectric cinstant (*a*), and Onsager function (*b*)

in the $XC_5H_4Ir(PH_3)_3$ iridabenzenes shows that dipole moment values increase with increasing Hammett constants. These calculations indicate higher β_{tot} values in the presence of electron donor groups. The NICS values are compatible with delocalized π electrons current.

REFERENCES

1. *Bleeke J.R.* // Chem. Rev. – 2001. – **101**. – P. 1205.
2. *He G., Xia H., Jia G.* // Chin. Sci. Bull. – 2004. – **49**. – P. 1543.
3. *Wright L.J.* // J. Chem. Soc., Dalton Trans. – 2006. – P. 1821.
4. *Chen J., Jia G.* // Coord. Chem. Rev. – 2013. – **257**. – P. 2491.
5. *Ghiasi R.* // Russ. J. Coord. Chem. – 2011. – **37**. – P. 72.
6. *Jacob V., Landorf C.W., Zakharov L.N., Weakley T.J.R., Haley M.M.* // Organometall. – 2009. – **28**. – P. 5183.
7. *Paneque M., Posadas C.M., Poveda M.L.* // J. Am. Chem. Soc. – 2003. – **125**. – P. 9898.
8. *Gilbertson R.D., Lau T.L.S., Lanza S.* // Organometall. – 2003. – **22**. – P. 3279.
9. *Gilbertson R.D., Weakley T.J.R., Haley M.M.* // J. Am. Chem. Soc. – 1999. – **121**. – P. 2597.
10. *Gilbertson R.D., Weakley T.J.R., Haley M.M.* // Chem. Eur. J. – **6**. – P. 437.
11. *Landorf C.W., Haley M.M.* // Angew. Chem., Int. Ed. – 2006. – **45**. – P. 3914.
12. *Fernandez I., Frenking G.* // Chem. Eur. J. – 2007. – **13**. – P. 5873.
13. *Iron M.A., Lucassen A.C.B., Cohen H., Boom M.E., Martin J.M.L.* // J. Am. Chem. Soc. – 2004. – **126**. – P. 11699.
14. *Rickard C.E.F., Roper W.R., Woodgate S.D., Wright L.J.* // Angew. Chem., Int. Ed. – 2000. – **39**. – P. 750.
15. *Clark G.R., Johns P.M., Roper W.R., Wright L.J.* // Organometall. – 2008. – **27**. – P. 451.
16. *Ghiasi R.* // Struct. Chem. – 2014. – **25**.
17. *Ghiasi R., Mokarram E.E.* // Russ. J. Coord. Chem. – 2011. – **37**. – P. 463.
18. *Clark G.R., Johns P.M., Roper W.R., Wright L.J.* // Organometall. – 2006. – **25**. – P. 1771.
19. *Clark G.R., Lu G.-L., Roper W.R., Wright L.J.* // Organometall. – 2007. – **26**. – P. 2167.
20. *Dalebrook A.F., Wright L.J.* // Organometall. – 2009. – **28**. – P. 5536.
21. *Wang T., Li S., Zhang H., Lin R., Han F., Lin Y., Wen T.B., Xia H.* // Angew. Chem., Int. Ed. – 2009. – **48**. – P. 6453.
22. *Frisch M.J., Trucks G.W., Schlegel H.B., Scuseria G.E., Robb M.A., Cheeseman J.R., Montgomery J.A. Jr., Vreven T., Kudin K.N., Burant J.C., Millam J.M., Iyengar S.S., Tomasi J., Barone V., Mennucci B., Cossi M., Scalmani G., Rega N., Petersson G.A., Nakatsuji H., Hada M., Ehara M., Toyota K., Fukuda R., Hasegawa J., Ishida M., Nakajima T., Honda Y., Kitao O., Nakai H., Klene M., Li X., Knox J.E., Hratchian H.P., Cross J.B., Adamo C., Jaramillo J., Gomperts R., Stratmann R.E., Yazyev O., Austin A.J., Cammi R., Pomelli C., Ochterski J.W., Ayala P.Y., Morokuma K., Voth G.A., Salvador P., Dannenberg J.J., Zakrzewski V.G., Dapprich S., Daniels A.D., Strain M.C., Farkas O., Malick D.K., Rabuck A.D., Raghavachari K., Foresman J.B., Ortiz J.V., Cui Q., Baboul A.G., Clifford S., Cioslowski J., Stefanov B.B., Liu G., Liashenko A., Piskorz P., Komaromi I., Martin R.L., Fox D.J., Keith T., Al-Laham M.A., Peng C.Y., Nanayakkara A., Challacombe M., Gill P.M.W., Johnson B., Chen W., Wong M.W., Gonzalez C., Pople J.A.* Gaussian 03, Revision B.03. – Pittsburgh, PA: Gaussian Inc., 2003.
23. *Krishnan R., Binkley J.S., Seeger R., Pople J.A.* // J. Chem. Phys. – 1980. – **72**. – P. 650.
24. *Wachters A.J.H.* // J. Chem. Phys. – 1970. – **52**. – P. 1033.
25. *Hay P.J.* // J. Chem. Phys. – 1977. – **66**. – P. 4377.
26. *McLean A.D., Chandler G.S.* // J. Chem. Phys. – 1980. – **72**. – P. 5639.
27. *Hay P.J., Wadt W.R.* // J. Chem. Phys. – 1985. – **82**. – P. 299.
28. *Hay P.J., Wadt W.R.* // J. Chem. Phys. – 1985. – **82**. – P. 284.
29. *Schaefer A., Horn H., Ahlrichs R.* // J. Chem. Phys. – 1992. – **97**. – P. 2571.
30. *Adamo C., Barone V.* // J. Chem. Phys. – 1998. – **108**. – P. 664.
31. *Reed A.E., Curtiss L.A., Weinhold F.* // Chem. Rev. – 1988. – **88**. –P. 899.
32. *Glendening E.D., Reed A.E., Carpenter J.E., Weinhold F.* NBO, 3.1. – Pittsburg, PA: Gaussian Inc., 2003.
33. *Chen Z., Wannere C.S., Corminboeuf C., Puchta R., Schleyer Pv.R.* // Chem. Rev. – 2005. – **105**. – P. 3842.
34. *Schleyer Pv.R., Marker C., Dransfeld A., Jiao H., Hommes N.J.R.V.* // J. Am. Chem. Soc. – 1996. – **118**. – P. 6317.
35. *Schleyer Pv.R., Monohar M., Wang Z., Kiran B., Jiao H., Puchta R., Hommes N.J.R.V.* // Org. Lett. – 2001. – **3**. – P. 2465.
36. *Corminboeuf C., Heine T., Seifert G., Schleyer Pv.R., Weber J.* // Phys. Chem. Chem. Phys. – 2004. – **6**. – P. 273.

37. *Fallah-Bagher-Shaidaei H., Wannere C.S., Corminboeuf C., Puchta R., Schleyer Pv.R.* // Org. Lett. – 2006. – **8**. – P. 863.
38. *Wolinski K., Hinton J.F., Pulay P.* // J. Am. Chem. Soc. – 1990. – **112**. – P. 8251.
39. *O'Boyle N.M., Tenderholt A.L., Langer K.M.* // J. Comput. Chem. – 2008. – **29**. – P. 839.
40. *Keleiman D.A.* // Phys. Rev. –1962. – **126**. – P. 1977.
41. *Runge E., Gross E.K.U.* // Phys. Rev. Lett. – 1984. – **52**. – P. 997.
42. *Tomasi J., Mennucci B., Cammi R.* // Chem. Rev. – 2005. – **105**. – P. 2999.
43. *Mendes P.J., Silva T.J.L., Carvalho A.J.P., Ramalho J.P.P.* // J. Mol. Struct.: THEOCHEM. – 2010. – **946**. – P. 33.
44. *Chen L.M., Chen J.C., Luo H. et al.* // J. Theor. Comput. Chem. – 2011. – **10**. – P. 581.
45. *Cao X., Liu C., Liu Y.* // J. Theor. Comput. Chem. – 2012. – **11**. – P. 573.
46. *Landorf C.W., Haley M.M.* // Angew. Chem., Int. Ed. – 2006. – **45**. – P. 3914.
47. *Onsager L.* // J. Am. Chem. Soc. – 1936. – **58**. – P. 1486.
48. *Clays K., Persoons A.* // Phys. Rev. Lett. – 1991. – **66**. – P. 2980.
49. *Lee H., An S.-Y., Cho M.* // J. Phys. Chem. B. – 1999. – **103**. – P. 4992.
50. *Ray P.C., Leszczynski J.* // Chem. Phys. Lett. – 2004. – **399**. – P. 162.